Metal Process Simulation Laboratory
Department of Mechanical and Industrial Engineering
University of Illinois at Urbana-Champaign
Urbana, IL 61801

Validation of CON1D Slab Surface Temperature Prediction Using Goodrich Pyrometer Measurements at Mittal Riverdale

By

Huan Li and Brian G. Thomas

Continuous Casting Consortium

Report

Submitted to

Mittal Steel
Goodrich Delavan

May 23, 2007

Objective

Three trials have been conducted at the thin-slab caster at Riverdale, Mittal Steel, where optical pyrometers from Goodrich are being implemented to measure temperature of the strand. Casting conditions are then input into CON1D to predict surface temperature. Comparisons are made with the Goodrich pyrometer measurements in order to validate both CON1D model and the accuracy of the pyrometer measurements at the Riverdale caster.

Trial 1: Sep. 11~12th, 2006

On Sep. 11, two Goodrich pyrometers were put below segment 2 (out of the spray zones). Pyrometer #1 is 8205mm below the meniscus, and Pyrometer #2 is 9731mm below meniscus. There is also a permanent fixed pyrometer (shear pyrometer) in Riverdale's caster, which is at the shear, i.e., 14550mm below meniscus.

Casting condition:

Since CON1D is a steady-state model, we choose two cases when the casting conditions reach a nearly steady state (for 20-50 minutes). With a machine length of 15m and casting speed of 4.5m/min, the minimum time needed to achieve steady-state casting after changing casting condition, is 15/4.5=3.4min. The main casting conditions for these two cases are shown in Table 1. The difference between cases is the pour temperature and the spray water flow rates.

Table 1 Casting conditions on Sep. 11th

	Case1 (12:07-13:40)	Case2 (13:50-14:40)
Casting condition:		
Casting speed (m/min):	4.445	4.445
Pour temperature (°C)	1551.7	1555
Slab thickness (mm)	55	55
Slab width (mm)	1451	1451
Distance of meniscus from top of mold (mm)	60	60
Working mold length (mm)	1040	1040
Nozzle submergence depth (mm)	300	300

Steel composition: (same for three cases, the property of this steel can be found in Appendix)		
C%	0.21	
Mn%	0.7	
S%	0.005	
P%	0.009	
Si%	0.04	
Cr%	0.03	
Ni%	0.03	
Cu%	0.03	
Mo%	0.02	
Ti%	0.002	
Al%	0.035	
%V	0.006	
%N	0.005	
Spray water flow rate (L/min/row):		
Water temperature (°C)	21.7	21.7
Zone 1	264.95	272.53
Zone 2	387.98	398.39
Zone 3	84.96	87.48
Zone 4	92.47	92.47
Zone 5	70.3	70.3
Mold cooling water:		
Water Temperature at mold top(°C)	23.9	23.9
Pressure (MPa)	1.413	1.413
Flowrate per wide face (L/s)	116.7	116.7
Cooling water temperature change(°C)	6.9	6.9

Pyrometer measurement:

The measured temperature of Goodrich pyrometers (#1 and #2) is shown in Figure 1. In order to compare with CON1D, the measured temperature is averaged over a period of time when the temperature can be considered steady state. Case1 temperatures are averaged from 12:40-13:40; and case2 from 13:50-14:15, which are shown in Figure 1. Temperature from shear pyrometer is obtained correspondingly from Riverdale caster monitor. Measured temperatures for each case are listed in Table 2.

Table 2 Measured temperatures from pyrometers

Case1						
pyrometer	#1(°F)	#2(°F)	shear(°F)	#1(°C)	#2(°C)	shear(°C)
max	1910	1990	1880	1043.3	1087. 8	1026. 7
min	1860	1910	1845	1015. 6	1043.3	1007.2
average	1887.6	1955.7	1862.5	1030. 9	1068.8	1016.9
Case2						
pyrometer	#1(°F)	#2(°F)	shear(°F)	#1(°C)	#2(°C)	shear(°C)
max	1920	1983	1880	1048. 9	1083. 9	1026.7
min	1860	1916	1850	1015. 6	1046. 7	1010.0
average	1886	1960	1865	1030.0	1071.3	1018.3

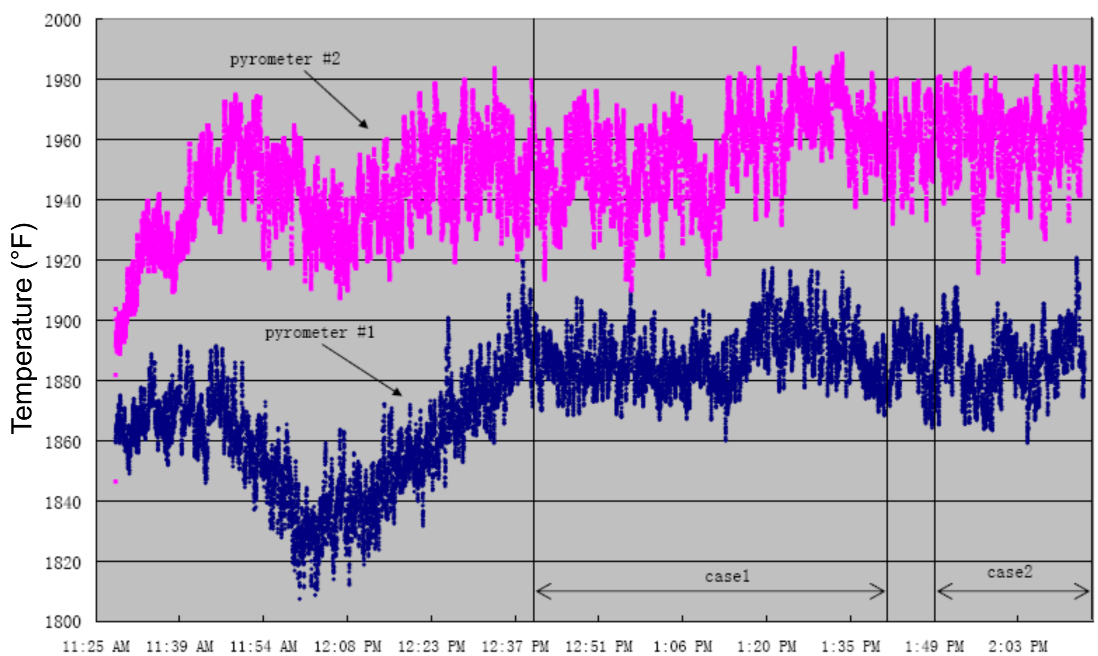

Figure 1 Temperature measurement from Goodrich pyrometers on Sep. 11th.

Simulation and comparison

Simulations are conducted for two casting conditions. The strand surface temperature predictions are compared with the pyrometer measurements, as shown in Figure 2.1~2.2 (a). Figs 2.1~2.2 (b) show the predicted shell thickness, solidus and liquidus locations. The temperature prediction is within the range of pyrometer measurement at pyrometer #2 and shear position, but is high (by 43°C and 38°C for case 1~2, respectively) at pyrometer #1. The reliability of pyrometer #1 is doubted. The position here is not far from segment 2. The water falls from upper spray zones and may generate much steam, which could make the measurement of pyrometer #1 much lower than the actual slab surface temperature.

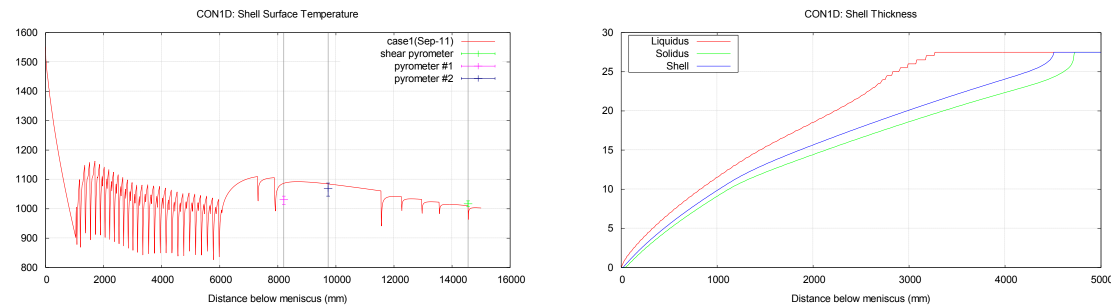

(a) Temperature prediction and comparison (b) Shell thickness prediction

Figure 2.1 Simulation results under casting condition case1(Sep-11)

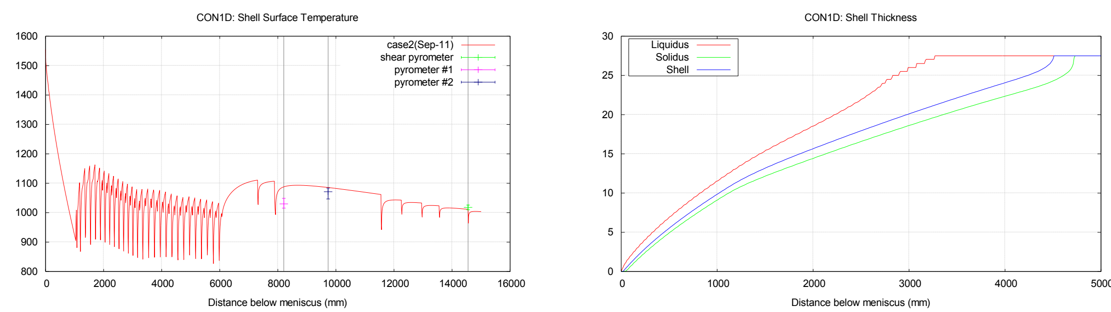

(a) Temperature prediction and comparison (b) Shell thickness prediction

Figure 2.2 Simulation results under casting condition case2(Sep-11)

Figure 3 compares the temperature prediction for the two cases. The predicted temperatures are observed to be almost the same (~1°C difference at pyrometer #1, #2 and shear location between two cases), due to the increasing water spray and also the increasing pour temperature from case1 to case2. The pyrometer measurements are also nearly unchanged between two cases (less than 3°C difference), as shown in Table 2, indicating the consistency of both the measurement and prediction.

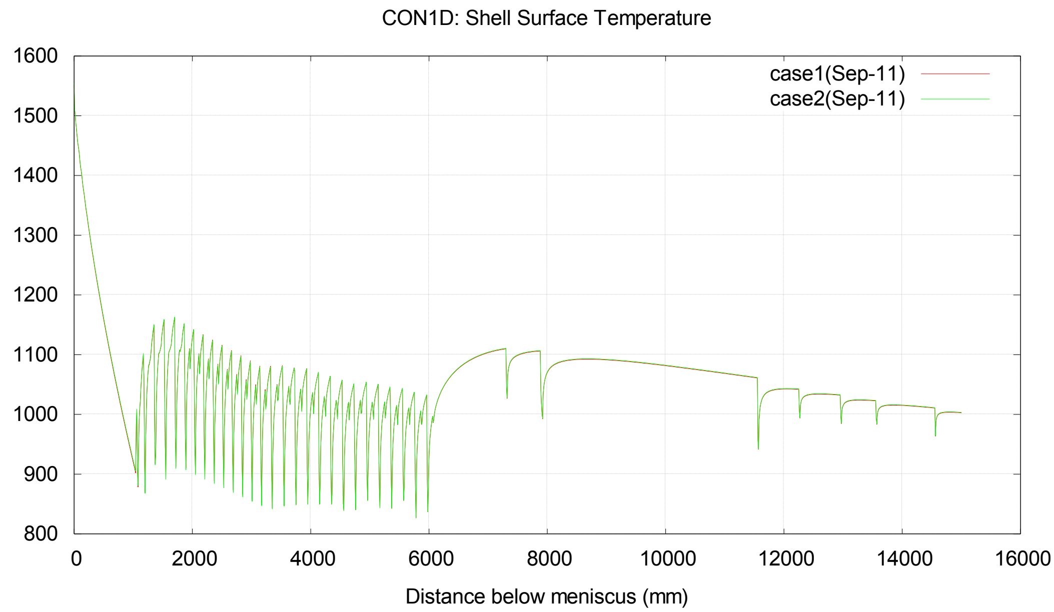

Figure 3 Difference of predicted temperature between two case1 and case2

Trial 2: Oct. 18~19th, 2006

On this trial, pyrometers from Goodrich didn't work. Hence, results are all from Riverdale's installed pyrometers. The locations of installed pyrometers are: pyrometer at the bend (bend pyrometer), 10256mm below the meniscus; pyrometer just before the shear-off (shear pyrometer), 14550mm below the meniscus.

Casting condition:

In this trial, we choose two cases when the casting conditions reach nearly steady state. Main casting conditions for these two cases are shown in Table 3. The differences between two cases are spray water flow rates, pour temperature and casting speed.

Table 3 Casting conditions on Oct. 19th

	Case3 (9:10-9:38)	Case4(9:45-10:25)
Casting condition:		
Casting speed (m/min):	4.47	4.34
Pour temperature (°C)	1554	1551
Slab thickness (mm)	55	55
Slab width (mm)	1451	1451
Distance of meniscus from top of mold (mm)	62	62

Working mold length (mm)	1040	1040
Nozzle submergence depth (mm)	316	316
Steel composition: same with steel composition in table 1		
Spray water flow rate (L/min/row):		
Water temperature (°C)	19.4	19.4
Zone 1	257.39	253.61
Zone 2	411.64	368.11
Zone 3	97.57	76.97
Zone 4	116.26	91.39
Zone 5	80.57	61.64
Mold cooling water (same for two cases):		
Water Temperature at mold top(°C)	41.7	
Pressure (MPa)	1.406	
Flowrate per wide face (L/s)	117.34	
Cooling water temperature change(°C)	6.9	

Pyrometer measurement:

Measured temperatures are obtained from bend pyrometer and shear pyrometer, as listed in Table 4.

Table 4 Measured temperatures from bend and shear pyrometer

Case3				
pyrometer	bend(°F)	shear(°F)	bend(°C)	shear(°C)
max	1950	1874	1066	1024
min	1914	1846	1046	1008
average	1932	1860	1056	1016
Case4				
pyrometer	bend(°F)	shear(°F)	bend(°C)	shear(°C)
max	2024	1898	1107	1037
min	1996	1870	1091	1021

average	2010	1884	1099	1029

Simulation and comparison

Figures below Fig. 4.1~4.2 are simulation results on Oct. 19th for case3 and case4. The strand surface temperature predictions are compared with the pyrometer measurements, as shown in Figure 4.1~4.2 (a). Figs 4.1~4.2 (b) show the predicted shell thickness, solidus and liquidus locations. In case3, the temperature prediction at bend is higher by 2°C than pyrometer measurement, and lower than measurement by 6°C at shear. In case4, the prediction is lower than the measurements by 20°C at bend and 18°C at shear.

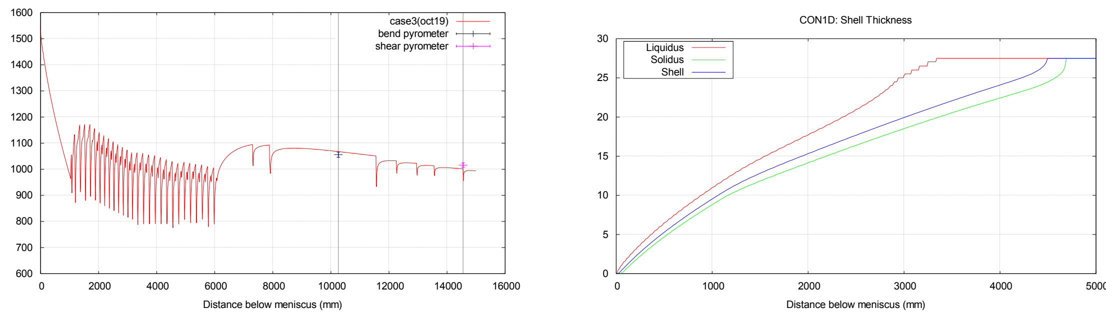

(a) Temperature prediction and comparison (b) Shell thickness prediction

Figure 4.1 Simulation results under casting condition case3 (Oct-19)

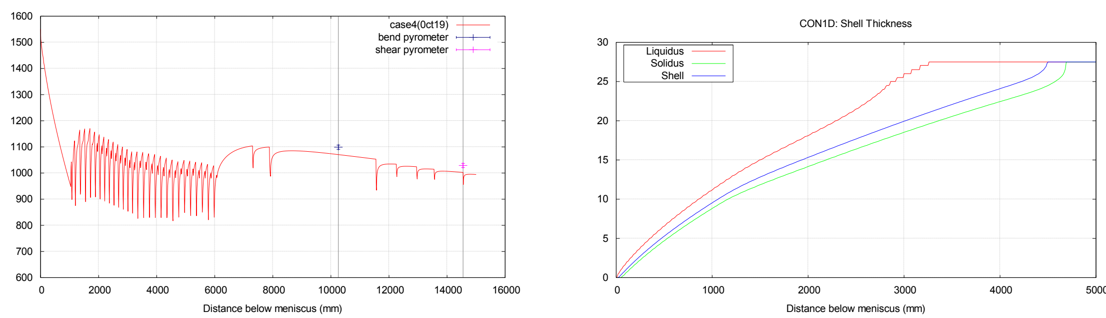

(a) Temperature prediction and comparison (b) Shell thickness prediction

Figure 4.2 Simulation results under casting condition case4 (Oct-19)

Figure 5 below shows the difference of temperature prediction between two cases. Although the casting speed is decreased from 4.47 to 4.34 m/min, which may decrease the temperature, the spray water is reduced much more. So, the predicted temperature increases (by 3°C at the bend, and 1°C at the shear).

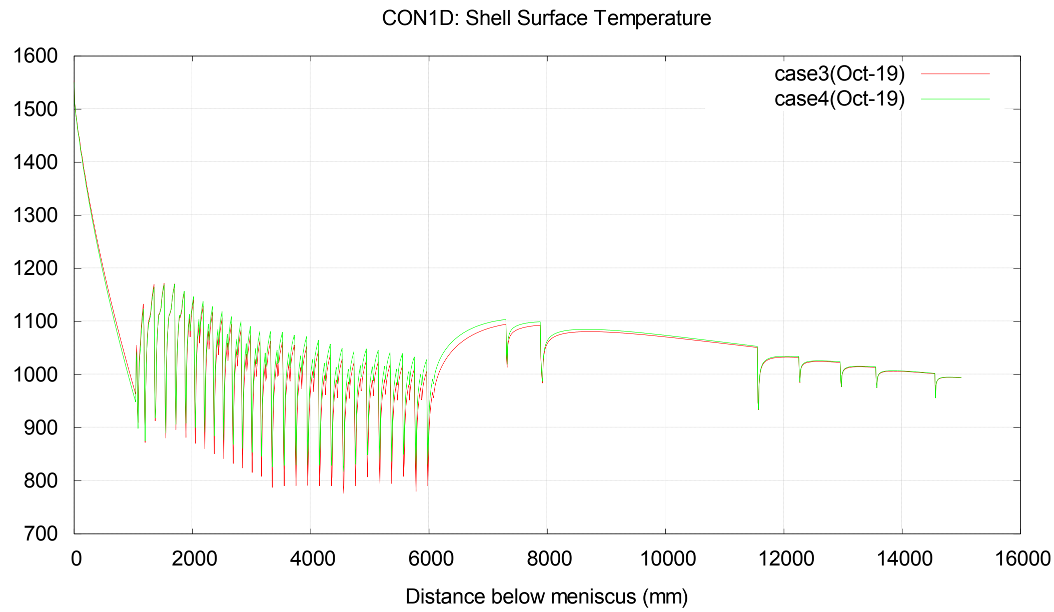

Figure 5 Difference of predicted temperature between case3 and case4

Trial 3: Mar. 12th, 2007

In the morning of Mar. 12th, three new Goodrich pyrometers were put in the same location of segment 2, 5361mm below meniscus. Bend and shear pyrometer are also at their locations same with trial 2.

Casting condition:

Table 5 Casting conditions on Mar. 12th

	Case5 (3:20-5:00)	Case6 (6:30-8:00)
Casting condition:		
Casting speed (m/min):	4.572	4.699
Pour temperature (°C)	1540	1549
Slab thickness (mm)	55	55
Slab width (mm)	1451	1451
Distance of meniscus from top of mold (mm)	60	60
Working mold length (mm)	1040	1040
Nozzle submergence depth (mm)	316	316

Steel composition: same with steel composition in table 1		
Spray water flow rate (L/min/row):		
Water temperature (°C)	19.4	19.4
Zone 1	276.32	283.89
Zone 2	378.52	448.55
Zone 3	78.65	104.30
Zone 4	90.84	116.26
Zone 5	62.19	88.68
Mold cooling water (same for two cases):		
Water Temperature at mold top(°C)	41.7	
Pressure (MPa)	1.427	
Flow rate per wide face (L/s)	117.1	
Cooling water temperature change(°C)	7.8	

Pyrometer measurement:

Three Goodrich optical pyrometers (two UV (#1, #2) and one IR (#3)) were in the same location of segment 2. One two-color-temperature is then obtained using one UV and one IR. Figure 6 and 7 below show the two-color-temperature T1 and T2, calculated from the measurements of pyrometer #1 and #3, pyrometer #2 and #3, respectively. The time over which the measured temperature is averaged, is shown in Figure 6 and Figure 7. Case 1 temperatures are averaged from 3:20-4:00; case2 from 6:30-7:40. Please note that the unit of temperature here has been converted to °C.

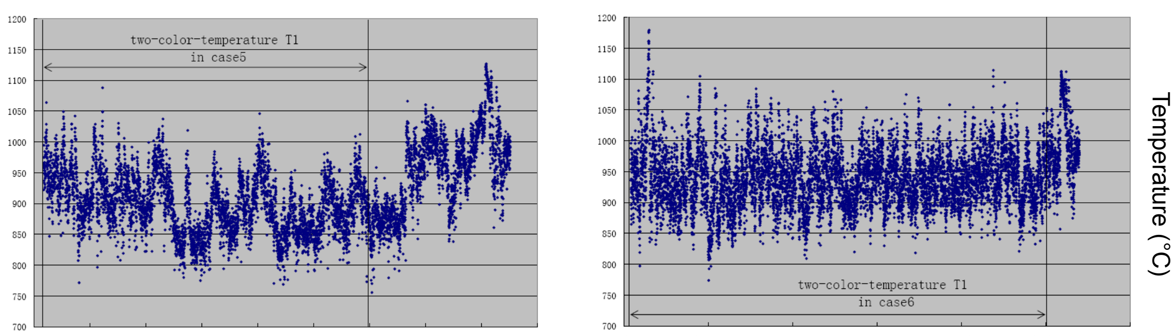

Figure 6 Two-color-temperature T1 from pyrometer #1 and #3

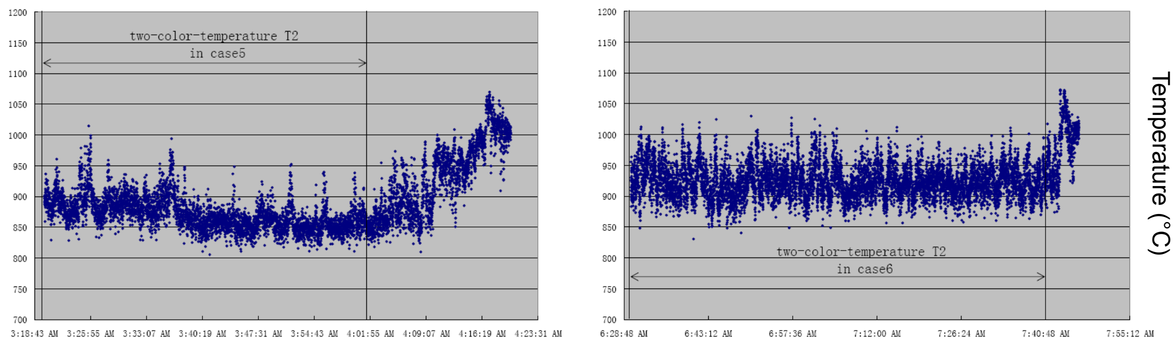

Figure 7 Two-color-temperature T2 from pyrometer #2 and #3

Measured temperatures from bend pyrometer and shear pyrometer can also be obtained from caster monitor. Measured temperatures at each case are listed in Table 6, which have already been converted to degree C.

Table 6 Measured temperatures from two-color-temperatures and Riverdale pyrometers

Case5				
pyrometer	T1(°C)	T2(°C)	bend(°C)	shear(°C)
max	1088	1014	1048.3	976.7
min	768	806	1029.4	932.2
average	915.0	890.0	1038. 9	953
Case6				
pyrometer	T1(°C)	T2(°C)	bend(°C)	shear(°C)
max	1180	1030	1053. 9	972.2
min	774	830	1048.3	938.8
average	942.6	927.5	1051.1	956.9

Simulation and comparison

Figures below Fig. 8.1~8.2 are simulation results on Mar. 12th for case5 and case6. Measurements of two Riverdale installed pyrometers (bend pyrometer and shear pyrometer) are compared with temperature prediction, as are shown in Fig. 8.1~8.2 (a). Two-color-temperatures T1 and T2 from Goodrich pyrometers are also compared with the surface temperatures computed by the CON1D model, as shown in close-up comparison in Figure 8.1~8.2 (c). The prediction of shell thickness, solidus and liquidus location is also shown in Figure 8.1~8.2 (b). In both two cases, the measurements of the Goodrich pyrometers inside the spray impinging region are very close to the prediction, between two temperature peaks of impinging region, as shown Figure 8.1~8.2 (c). The measurements at shear and bend pyrometers are lower than prediction, by 40°C and 21°C at the bend, 43°C and 41°C at the shear, for case5 and case6, respectively.

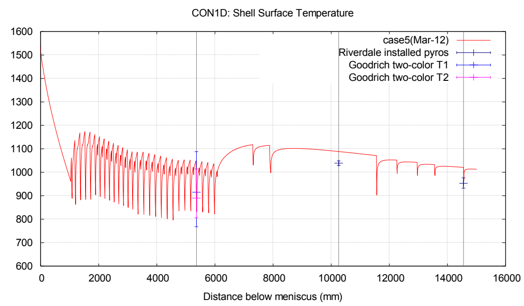

(a) Temperature prediction and comparison

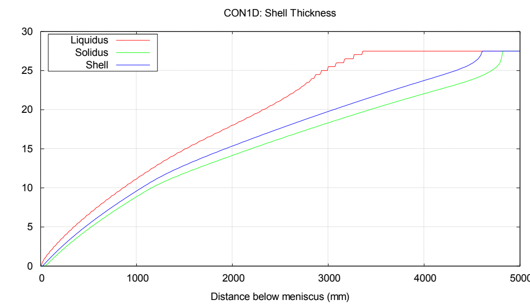

(b) Shell thickness prediction

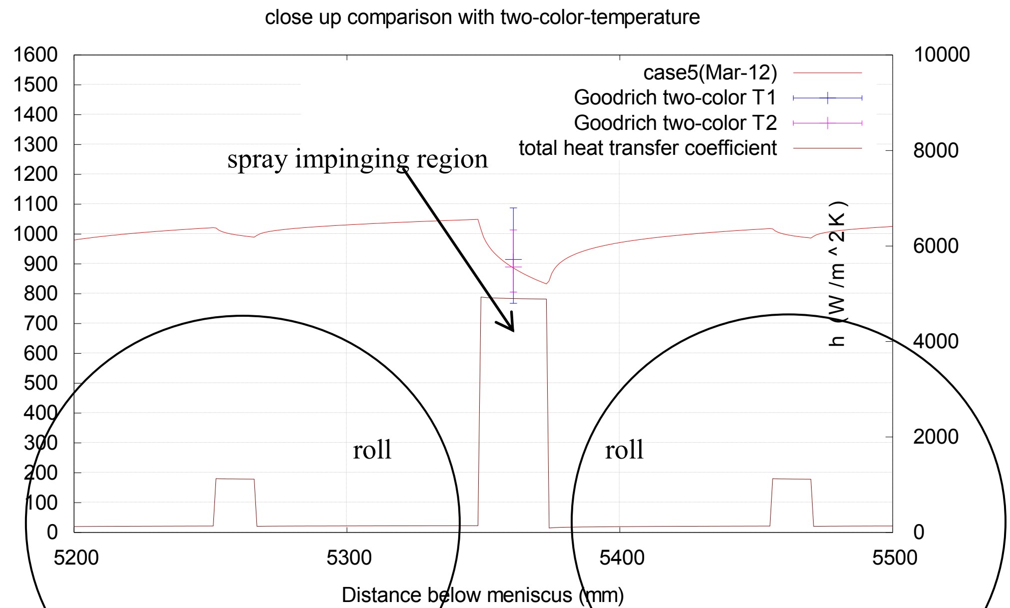

(c) close up comparison with two-color-temperature

Figure 8.1 Simulation results under casting condition case5 (Mar-12)

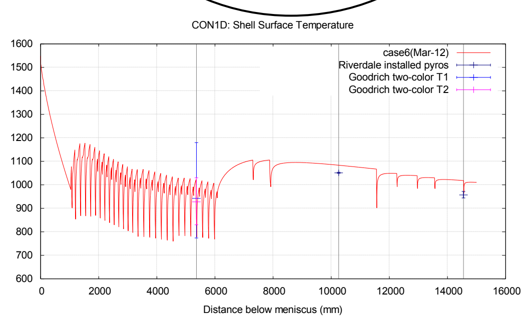

(a) Temperature prediction and comparison

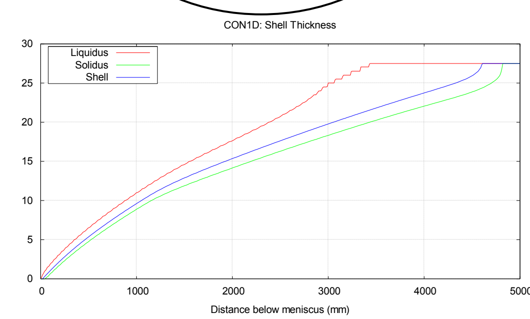

(b) Shell thickness prediction

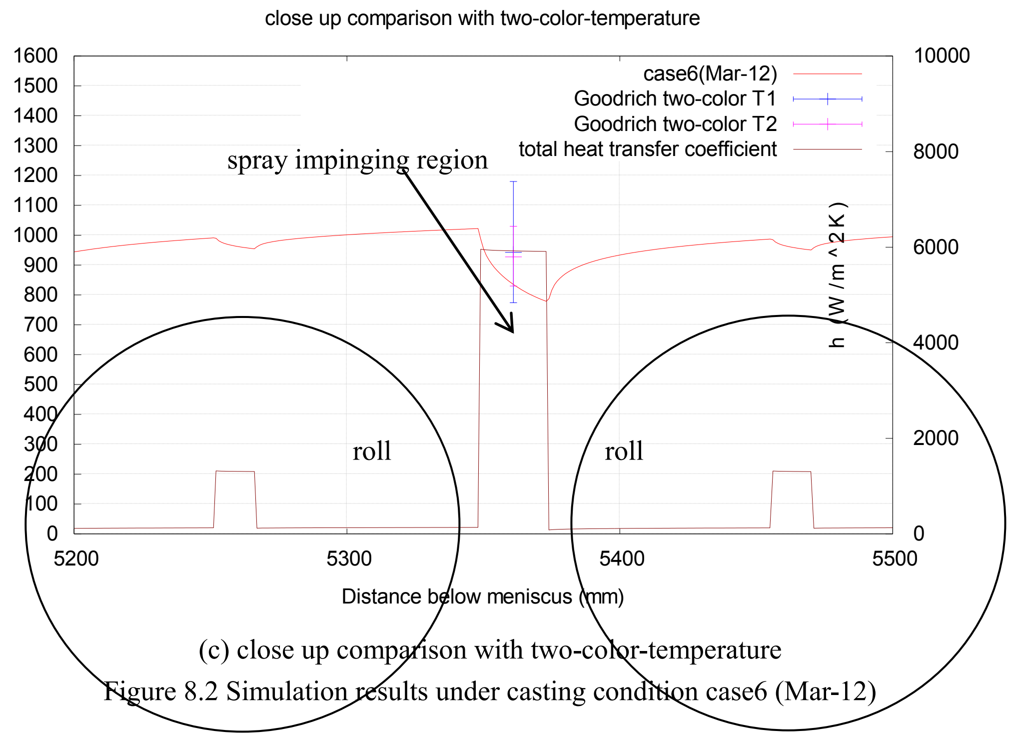

(c) close up comparison with two-color-temperature

Figure 8.2 Simulation results under casting condition case6 (Mar-12)

Figure 9 below shows the difference of temperature prediction for two cases. From case5 to case6, although the casting speed and pour temperature increase, which will raise the temperature, the spray water is rising more significantly. Hence, the predicted temperature drops (by 50°C at two-color-temperature pyrometer position, 5°C at the bend and 3°C at the shear).

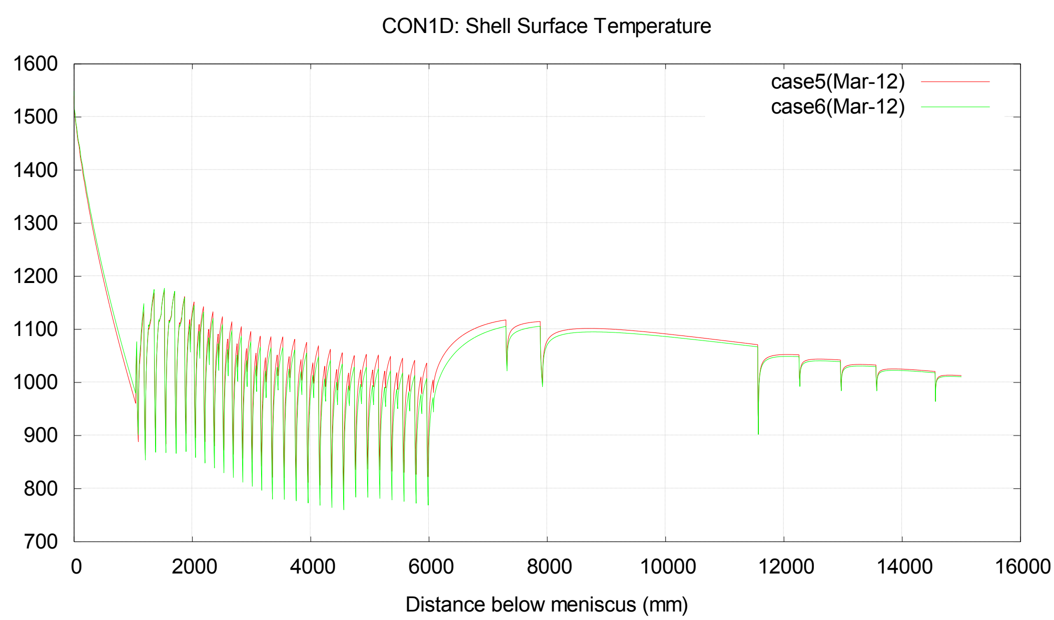

Figure 9 Difference of predicted temperature between two cases

Conclusion:

Plant trials at Mittal Riverdale generated pyrometer temperature data for several different sets of casting conditions (case1~case6), which were also modeled with CON1D for comparison. Pyrometer measurements varied by 20°C between different two-color methods and 200°C over 90 minutes time intervals of roughly steady casting. The model temperature predictions are generally reasonable for most casting conditions, being 1°C-43°C higher than the pyrometers, (except for case3 at the shear position and case4). However, there are some interesting discrepancies for some cases. Specifically, increasing water flow rate (by ~25%) in trial 3 caused an increase in measured strand temperature (of 30°C in the strand, 13°C at the bend, and 3°C at the shear), which was not expected in the model. The model predicted decreases of 50°C, 5°C, and 3°C. It is possible that this reversal of expectations might be due to creating a gas / water film barrier that decreased heat extraction with increasing water flow, which is related to the Leidenfrost effect. Theoretical calculations should be performed to investigate this, and the measurements from Cinvestav, Mexico should be incorporated. In addition, the fraction of heat extracted by different rolls might vary with casting conditions such as water flow rate, and requires investigation.

Alternatively, the stability, consistency and repeatability of pyrometer measurements greatly influence the reliability of the comparison. Thus, further investigation of the accuracy of the pyrometer measurements is also recommended, both for calibrating our model and for monitoring the caster.

Appendix

All the simulation results are calculated by CON1D-8.0. A sample input file and an output file which includes the steel property are attached. Other output files are too long and not included here. Those files can be obtained simply by running CON1D with the input file. To get case2~case6 input files, use Table 1, Table 3 and Table 5 to change the corresponding data in the input file.

[1]. CON1D input file, case1.inp

[2]. CON1D output file, case1.ext

[1] CON1D input file, case1.inp

```
CON1D-8.0 Slab Casting Heat Transfer Analysis
             University of Illinois, Brian G. Thomas, 2004
Mittal Riverdale and Goodrich Delavan. May-2007
INP                         Input Data                           INP

 (1) CASTING CONDITIONS:
         1      Number of time-cast speed data points
                (If=1, constant casting speed)
                Next 2 lines contain time(s) and vc(m/min) data points
   0.
 4.445
  1551.700       Pour temperature (C)
  55.0000       Slab thickness (mm)
  1451.240       Slab width (mm)
  60.0000       Distance of meniscus from top of mold (mm)
  1040.0000       Working mold length (mm)
  300.0000       Z-distance for heat balance  (mm)
  300.0000       Nozzle submergence depth (mm)

 (2) SIMULATION PARAMETERS:
         0      Which shell to consider? (0=wide face; 1=narrow face)
         1      What type of mold? (0=slab, 1=funnel mold, 2=billet mold)
         2      Which moldface to consider? (0=outer, 1=inner, 2=straight)
         -1      Calculate mold and interface (=0 flux casting, or 2 oil casting )
                or enter interface heat flux data (=-1)
        2      Number of zmm and q data points (if above = -1)
                Next 2 lines contain zmm(mm) and q(kW/m2) data
    0.   1100.
  2552.96  2552.96
  0.0000000E+00   Is superheat treated as heatflux?
                0=no; 1=yes (take default); -1=yes (enter data)
        17      Number of zmm and q data points(if above = -1)
                Next 2 lines contain zmm(mm) and q(kW/m2) data
   10.    45.   100.   200.   300.   400.   500.   675.   720.   770.   980.  1120.  1370.  1470.
1575.  1700.  2000.
   20.    40.    58.    57.    28.    36.    88.   384.   408.   406.   321.   303.    98.    58.    38.
25.    20.
         1      Do you want (more accurate) 2d calculations in mold?
                (0=no; 1=yes; 2=yes, one extra loop for better taper)
  200.0000       Max. dist. below meniscus for 2d mold calcs (mm)
                (=mold length if above = 2)
  1.0E-03   Time increment (s)
       55      Number of slab sections
  10.00000       Printout interval (mm)
  0.0000000E+00   Start output at (mm)
  15000.000       Max. simulation length (must > z-distance)(mm)
  27.50000       Max. simulation thickness (mm)
                (smaller of max. expected shell thickness &
                half of slab thickness)
     800000      Max. number of iterations
         3      Shell thermocouple numbers below hot face (less than 10)
                Next line gives the distance below surface of thermocouples(mm)
   10.0   12.5   25.0
  0.7000000       Fraction solid for shell thicknesss location (-)

 (3) STEEL PROPERTIES:
 0.2100 0.7000 0.0050 0.0090 0.0400    %C ,%Mn,%S ,%P ,%Si
 0.0300 0.0300 0.0300 0.0200 0.0020    %Cr,%Ni,%Cu,%Mo,%Ti
 0.0350 0.0060 0.0050 0.0000 0.0000    %Al,%V ,%N ,%Nb,%W
 0.0000                                %Co,(additional components)
      1000      Grade flag
                (1000,304,316,317,347,410,419,420,430,999)
         1      If CK simple Seg. Model wanted for default Tliq,Tsol
                (1=yes,0=no)
  10.00000       Cooling rate used in Seg.Model(if above =1) (K/sec)
                Override defaults with following constants(-1=default)
```

```
 -1.000000       Steel liquidus temperature (C)
 -1.000000       Steel solidus temperature (C)
 -1.000000       Steel density (g/cm^3)
 -1.000000       Heat fusion of steel (kJ/kg)
 -1.000000       Steel emissivity (-)
 -1.000000       Steel specific heat (kJ/kg deg K)
 -1.000000       Steel thermal conductivity (W/mK)
 -1.000000       Steel thermal expansion coeff. (/K)

(4) SPRAY ZONE VARIABLES:
  26.61         Water and ambient temperature after spray zone(Deg C)
               spray zone condition:(heat tran.coeff.funct:h=A*C*W^n(1-bT))
               (Nozaki Model:A*C=0.3925,n=0.55,b=0.0075)
  1.570000       A(0=off)
 0.5500000       n
 7.4999998E-03    b
  8.700000       minimum convection heat trans. coeff. (natural) (W/m^2K)
        12      Number of zones
No.  zone    rol.     water       spray     contct frac.of   spray   conv    amb.
   starts  #  rad.   flowrate   width  length  angle  q thr rol coeff   coeff   temp.
    (mm)      (m)  (l/min/row)   (m)    (m)    (Deg)                (W/m^2K)  (DegC)
 1  1040.0   1  0.02    264.95    1.626  0.0254    3.00   0.00    0.25   8.70    20.56
 2  1105.0   4  1.00    387.02    1.258  0.0254    2.26   0.1     0.25  8.70    20.56
 3  1800.0   9  0.060   84.96     0.760  0.0254    10.00  0.1     0.4    8.70    20.56
 4  3240.0   7  0.0825  92.47     0.760  0.0254    10.00  0.1     0.4    8.70    20.56
 5  4647.0   7  0.0825  70.30     0.760  0.0254    10.00  0.1     0.4    8.70    20.56
 6  6075.0   1  0.02    0.0000    1.422  0.0254    3.00   0.00    0.60   8.70    20.56
 7  7300.0   1  1.00    0.0000    1.422  0.0254    2.26   0.50    0.50   8.70    20.56
 8  7900.0   1  0.060   0.0000    1.422  0.0254    10.00  0.120   0.5    8.70    20.56
 9  11562.   1  0.0825  0.0000    1.422  0.0254    10.00  0.200   0.50   8.70    20.56
 10 12262.   1  0.0825  0.0000    1.422  0.0254    10.00  0.200   0.50   8.70    20.56
 11 12962.   1  0.0825  0.0000    1.422  0.0254    10.00  0.200   0.50   8.70    20.56
 12 13562.   1  0.0825  0.0000    1.422  0.0254    10.00  0.200   0.50   8.70    20.56
    14562.    End of last spray zone (mm)

(5) MOLD FLUX PROPERTIES:
36.70 40.80  3.60  2.16  0.65    %CaO,%SiO2,%MgO,%Na2O,%K2O
 0.00  0.70  0.00  1.26  0.00    %FeO,%Fe2O3,%NiO,%MnO,%Cr2O3
 5.60  0.00  0.00  0.00  0.00    %Al2O3,%TiO2,%B2O3,%Li2O,%SrO
 0.00  0.00  0.00  0.00  0.00    %ZrO2,%F,%free C,%total C,%CO2
        1      number of Tfsol and viscosity exponent n
               Next 3 lines contain zmm(mm) and tfol and expn data
   0.
1120.00
 1.650
  1.500000       Solid flux conductivity(W/mK)
        1      number of Liquid flux conductivity data
               Next 2 lines contain zmm and Tkliquid data
   0.
 1.500
 0.8300000       Flux viscosity at 1300C (poise)
  2500.000       Mold flux density(kg/m^3)
  250.0000       Flux absorption coefficient(1/m)
  1.500000       Flux index of refraction(-)
              (-1 = take default f(composition)
 0.9000000       Slag emissivity(-)
        2      Form of mold powder consumption rate(1=kg/m^2; 2=kg/t)
 0.2500000       Mold powder consumption rate
 0.0000000E+00    Location of peak heat flux (m)
 2.0000000E-10    Slag rim thickness at metal level (meniscus) (mm)
 2.0000000E-10    Slag rim thickness at heat flux peak (mm)
  10.00000       Liquid pool depth (mm)
  80.00000       Solid flux tensile fracture strength (KPa)
  8000.000       Solid flux compress fracture strength (KPa)
 0.1700000       Solid flux Poisson ratio(-)
        1      number of slag static friction coeff data
               Next 2 lines contain zmm and Static friction coeff
   0.
```

```
 0.500
 0.5000000      Moving friction coefficient between solid flux and mold wall

(6) INTERFACE HEAT TRANSFER VARIABLES:
        1      Number of distance-vratio data points
               (1=constant ratio of solid flux velocity
               to casting speed)
               Next 2 lines contain zmm(mm) and ratio(-) data
   0.
0.010
 5.0000000E-09   Flux/mold or shell/mold contact resistance(m^2K/W)
 0.5000000      Mold surface emissivity(-)
 5.9999999E-02   Air conductivity(in oscillation marks)(W/mK)
        0      Osc.marks simulation flag(0=average,1=transient)
 0.2500000      Oscillation mark depth(mm)
  4.500000      Width of oscillation mark (mm)
  1.388889      Oscillation frequency(cps)
               (-1=take default cpm=2*ipm casting speed)
  7.800000      Oscillation stroke(mm)

(7) MOLD WATER PROPERTIES:
 -1.000000      heat transfer coefficient(W/m^2K)
               (-1=default=f(T), based on Sleicher and Rouse Eqn)
  4179.000      Water heat capacity(J/kgK)(-1=default=f(T))
  995.6000      Water density(kg/m3)(-1=default=f(T))

(8) MOLD GEOMETRY:
  30.00000      WF Mold thickness with water channel (mm),(outer rad.,top)
  30.00000      WF Mold thickness with water channel (mm),(inner rad.,top)
  22.00000      Narrow face (NF) mold thickness with water channel (mm)
  70.00000      Equivalent thickness of water box (mm)
 -1.000000      Mean temperature diff between hot & cold face of NF (C)
  6.00000     15.00000    Cooling water channel depth(mm)(WF,NF)
  25.000000     5.000000    Cooling water channel width(mm)(WF,NF)
  40.00000     20.00000    Channel distance(center to center)(mm)(WF,NF)
 -1.000000    -1.000000    Total channel cross sectional area(mm^2)(WF,NF)
                          (served by water flow line where temp rise measured)
  350.0000     350.0000    Mold thermal conductivity(W/mK)(WF,NF)
 1.6000000E-05   Mold thermal expansion coeff. (1/K)
  23.89000      Cooling water temperature at mold top(C)
    1.413      Cooling water pressure(MPa)
        2      Form of cooling water velocity/flowrate(1=m/s ; 2=L/s)
  116.7042     116.7042    Cooling water velocity/flowrate per face (WF,NF)
                          (> 0 cooling water from mold top to bottom
                          < 0 cooling water from mold bottom to top)
  850.0000      funnel height (mm)
  1100.000      funnel width (mm)
  60.00000      funnel depth at mold top (mm)
  10.38500      Machine outer radius(m)
  10.18500      Machine inner radius(m)
        2      Number of mold coating/plating thickness changes down mold
  No.  Scale     Ni      Cr     Others  Air gap   Z-positions  unit
  1    0.000   0.000   0.000    0.000    0.000      0.000      (mm)
  2    0.000   0.000   0.000    0.000    0.000    1040.000      (mm)
       0.550  72.100  67.000    1.000    0.060   Conductivity  (W/mK)

(9) MOLD THERMOCOUPLES: (not considered in this study)
        8      Total number of thermocouples
No.    Distance beneath    Distance below
       hot surface(mm)     meniscus(mm)
   1     14.00              50.00
   2     14.00              50.00
   3     14.00             150.00
   4     14.00             150.00
   5     15.40             170.00
   6     14.00             170.00
   7     13.80             370.00
   8     14.00             370.00
```

[2] CON1D output file including steel property, case1.ext

```
            CON1D-8.0 Slab Casting Heat Transfer Analysis
            University of Illinois, Brian G. Thomas, 2004

EXIT                Calculated Conditions                          EXT


     Initial casting speed:                    74.08    (mm/s)
     Carbon content:                          0.2100    (%)
     Wide face simulation:

 Steel Properties:
     The following 3 temperature from Y.M.Won Segregation Model
     Liquidus Temp:                          1514.60    Deg C
     Solidus Temp:                           1466.09    Deg C
     Peritectic Temp:                        1494.62    Deg C

     AE3 Temp:                               810.75    Deg C
     AE1 Temp:                               724.67    Deg C

 Parameters Based on Derived Mold Values:
     Carbon equivalent:                       0.3419    (%)
     (using initial casting speed:)
      Negative strip time:                      0.00    (s)
      Positive strip time:                      0.72    (s)
      Velocity amplitude of mold oscillation:     34.03   (mm/s)
      Pitch(spacing betweeen oscillation marks):   53.34    (mm)
      % Time negative strip:                     0.00    (%)
      Average percent negative strip velocity:   -70.75    (%)

     Cooling water velocity:                   21.44    (m/s)
     Cooling water flow rate per face:        116.7042    (L/s)
     Average mold flux thickness:              0.0066    (mm)
     (based on consumption rate)
     (assuming flux moves at casting speed)
     min. heat trans. coeff. on mold cold face    46.55    kW/m2K
     max. heat trans. coeff. on mold cold face    61.75    kW/m2K
     Water boiling temperature:               150.000    Deg C
     Max cold face temperature:                73.161    Deg C
     Max hot face temperature(copper only):     248.221    Deg C
     Max hot face temperature(w/coating):      248.221    Deg C
     Mold water temp diff(in hot channel):      7.9249    Deg C
     Mold water temp diff over all channels is not available
     Mean heat flux in mold:                  2552.97    (kW/m^2)

 Friction Values:
     Average absolute shear stress in Mold:      0.0000    (kPa)
     Average friction force in Mold:           0.0000    (kN)
     Max. shear stress in Mold:               0.0000    (kPa)
     Max friction force in Mold:              0.0000    (kN)
     Min. shear stress in Mold:               0.0000    (kPa)
     Min friction force in Mold:              0.0000    (kN)
     shear stress in Mold when Vmold=0:         0.0000    (kPa)
     Friction force in Mold when Vmold=0:        0.0000    (kN)
     Calculated solid flux velocity ratio       0.0000    (-)
     Calculated solid flux consumption:      0.000E+00    (m^2)
     Used solid flux consumption:           0.000E+00    (m^2)
     Calculated liquid flux consumption:      0.000E+00    (m^2)
     Used liquid flux consumption:          0.000E+00    (m^2)
     Used osc. flux consumption:            0.000E+00    (m^2)

 Heat Balance at  300.04mm:
     Heat Extracted:                          10.34    (MJ/m^2)
     Heat Input to shell inside:                0.00    (MJ/m^2)
     Super Heat:                              1.77    (MJ/m^2)
```

Latent Heat in mushy region: 1.15 (MJ/m^2)
Latent Heat in Solid region: 5.51 (MJ/m^2)
Sensible Cooling: 2.08 (MJ/m^2)
Total Heat: 10.52 (MJ/m^2)
Error In Heat Balance: 1.74 (%)

Heat Balance at Mold Exit(1040.04mm):

Heat Extracted:	35.84	(MJ/m^2)
Heat Input to shell inside:	0.00	(MJ/m^2)
Super Heat:	3.65	(MJ/m^2)
Latent Heat in mushy region:	1.43	(MJ/m^2)
Latent Heat in Solid region:	18.55	(MJ/m^2)
Sensible Cooling:	13.04	(MJ/m^2)
Total Heat:	36.66	(MJ/m^2)
Error In Heat Balance:	2.29	(%)

Variables Calculated at Mold Exit(1040.04mm):

taper (per mold, narrow face):	0.76	(%)
taper (per mold per length, narrow face):	0.73	(%/m)
Shell thickness:	9.94	(mm)
Liquid flux film thickness:	0.0000	(mm)
Solid flux film thickness:	0.0000	(mm)
Total flux film thickness:	0.0000	(mm)
Shell surface temperature:	902.21	Deg C
Mold hot face temperature:	248.22	Deg C
Heat flux:	2.5530	(MW/m^2)

Predicted Thermocouple Temperatures:

No.	distance beneath hot surface(mm)	distance below meniscus(mm)	temperature Deg C
1	14.00	50.00	136.45
2	14.00	50.00	136.45
3	14.00	150.00	141.63
4	14.00	150.00	141.63
5	15.40	170.00	131.50
6	14.00	170.00	141.71
7	13.80	370.00	144.20
8	14.00	370.00	142.74